Acarbose Rearrangement Mechanism Implied by the Kinetic and Structural Analysis of Human Pancreatic α-Amylase in Complex with Analogues and Their Elongated Counterparts[†,‡]

Chunmin Li,[§] Anjuman Begum,[§,||] Shin Numao,[||,⊥] Kwan Hwa Park,[@] Stephen G. Withers,[§,⊥] and Gary D. Brayer*[,§]

Department of Biochemistry and Molecular Biology, University of British Columbia, Vancouver, British Columbia V6T 1Z3, Canada, Department of Chemistry, University of British Columbia, Vancouver, British Columbia V6T 1Z1, Canada, and Research Center for New Bio-Materials in Agriculture and Department of Food Science and Technology, Seoul National University, Seoul 151-921, Korea

Received August 3, 2004; Revised Manuscript Received November 1, 2004

ABSTRACT: A mechanistic study of the poorly understood pathway by which the inhibitor acarbose is enzymatically rearranged by human pancreatic α-amylase has been conducted by structurally examining the binding modes of the related inhibitors isoacarbose and acarviosine-glucose, and by novel kinetic measurements of all three inhibitors under conditions that demonstrate this rearrangement process. Unlike acarbose, isoacarbose has a unique terminal α-(1−6) linkage to glucose and is found to be resistant to enzymatic rearrangement. This terminal glucose unit is found to bind in the +3 subsite and for the first time reveals the interactions that occur in this part of the active site cleft with certainty. These results also suggest that the +3 binding subsite may be sufficiently flexible to bind the α-(1−6) branch points in polysaccharide substrates, and therefore may play a role in allowing efficient cleavage in the direct vicinity of such junctures. Also found to be resistant to enzymatic rearrangement was acarviosine-glucose, which has one fewer glucose unit than acarbose. Collectively, structural studies of all three inhibitors and the specific cleavage pattern of HPA make it possible to outline the simplest sequence of enzymatic reactions likely involved upon acarbose binding. Prominent features incorporated into the starting structure of acarbose to facilitate the synthesis of the final tightly bound pseudo-pentasaccharide product are the restricted availability of hydrolyzable bonds and the placement of the transition state-like acarviosine group. Additional "*in situ*" experiments designed to elongate and thereby optimize isoacarbose and acarviosine-glucose inhibition using the activated substrate αG3F demonstrate the feasibility of this approach and that the principles outlined for acarbose rearrangement can be used to predict the final products that were obtained.

Human α-amylase catalyzes the hydrolysis of α-(1−4) glycosidic linkages in glucose polymers such as starch. Overall, digestion of starch occurs in several stages. An initial, limited digestion is provided by the salivary α-amylase, which degrades polymeric starch to shorter oligomers. Upon reaching the digestive system, starch is further extensively hydrolyzed by the α-amylase produced in the pancreas and excreted into the lumen. The resultant oligosaccharide mixture, including maltose, maltotriose, and a number of other α-(1−6) and α-(1−4) oligoglucans, is then degraded to glucose by other α-glucosidases. The glucose that is produced is then absorbed and enters the bloodstream by means of a specific transport system.

Both the human salivary (HSA)[1] and pancreatic (HPA) α-amylase isozymes are composed of 496 amino acids in a single polypeptide chain and bind essential chloride and calcium ions (*3*−*5*). These are encoded as part of a multigene family on chromosome 1 and regulated so that the different isozymes are expressed solely in either the salivary glands or the pancreas (*6*). The sequences of these two isozymes are ∼97% identical (*7*), though some of the 15 amino acid substitutions between them occur in the active site region, resulting in somewhat different cleavage patterns (*2*). A high level of homology is also found for their tertiary structures, with both isozymes found to be composed of three structural domains (*2*, *8*). Domain A is the largest and forms an eight-stranded parallel β-barrel. It is here that the three active site residues (D197, E233, and D300) are located, along with the chloride binding site. Domain B forms the calcium binding site, which is positioned adjacent to the wall of the β-barrel of domain A. Domain C is only loosely associated with the other two domains and is of unknown function.

[†] This work was supported by an operating grant from the Canadian Institutes of Health Research (CIHR).

[‡] Coordinates for the structures described in this work have been deposited in the Protein Data Bank (*1*). The following PDB file names have been assigned: 1XCX for the isoacarbose complex, 1XD1 for the αG3F−isoacarbose complex, 1XCW for the acarviosine-glucose compex and 1XD0 for the α-G3F−acarviosine-glucose complex.

* To whom correspondence should be addressed. Telephone: (604) 822-5216. Fax: (604) 822-5227. E-mail: brayer@interchange.ubc.ca.

[§] Department of Biochemistry and Molecular Biology, University of British Columbia.

[||] These authors contributed equally to this work.

[⊥] Department of Chemistry, University of British Columbia.

[@] Seoul National University.

[1] Abbreviations: HPA, human pancreatic α-amylase; HSA, human salivary α-amylase; Iacb, isoacarbose; Acg, acarviosine-glucose; αG3F, α-maltotriosyl fluoride; αCNP-G3, 2-chloro-4-nitrophenyl α-maltotrioside. Amino acid numbering is according to a sequence alignment of HPA (*2*).

10.1021/bi048334e CCC: $30.25
Published on Web 02/10/2005

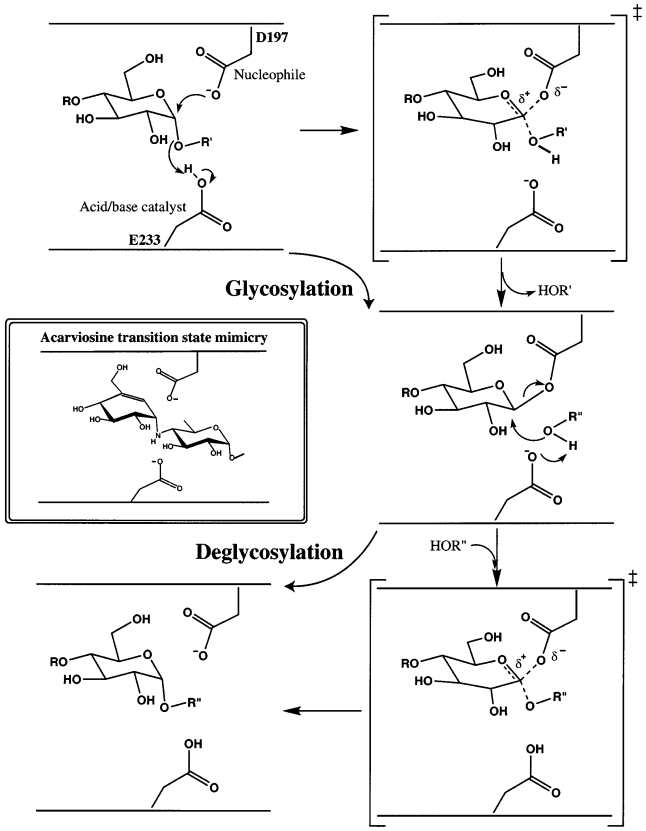

FIGURE 1: Schematic representation of the catalytic mechanism of HPA. R″ in this case can represent the hydrogen of a water molecule in a hydrolysis reaction, or alternatively, it can represent some other sugar residue which in this case would lead to a transglycosylation reaction. Shown in the double-boxed panel is the common conformation observed for the acarviosine group of acarbose, isoacarbose, and acarviosine-glucose, as bound in the active site of HPA. It is believed that this group mimics the transition state occurring during the first step of catalysis. The N-linked glycosidic bond of this group cannot be cleaved by HPA.

Of the sequence-related groupings assembled for glycosidases, the human α-amylases belong to family 13 (*9*, *10*). As in this family of enzymes, hydrolysis of substrates occurs with net retention of configuration at the sugar anomeric center (*11*), and is believed to proceed via a double-displacement mechanism involving the formation and hydrolysis of a covalent *β*-glycosyl−enzyme intermediate (Figure 1). Formation of this intermediate involves attack at the sugar anomeric center by the catalytic nucleophile D197 (*12*). This is assisted by general acid catalysis believed to be provided by E233 (*13*). The covalent glycosyl−enzyme intermediate that is formed then undergoes general base-catalyzed hydrolysis via attack of water at the anomeric center. As indicated in Figure 1, it is proposed that this catalytic mechanism proceeds via oxocarbenium ion-like transition states.

Considerable effort has been expended in the search for and development of inhibitors of starch digestion for use as potential therapeutics for human conditions such as diabetes and obesity (*14*−*22*). For HPA, one of the most successful examples of such inhibitors is acarbose, a natural product isolated from *Streptomyces* sp. (see Figure 2). This is a pseudo-tetrasaccharide composed of maltose bound to an acarviosine group. The valienamine (unsaturated cyclitol) and 4,6-dideoxyglucose moieties of acarviosine are linked through a nitrogen atom, and therefore, this bond cannot be cleaved

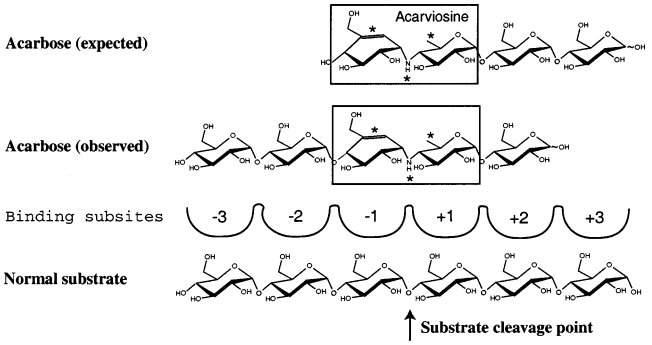

FIGURE 2: Schematic drawing of the structure of acarbose and its expected mode of binding to HPA. Shown below is the observed structure of acarbose as bound to HPA after having been enzymatically rearranged through a series of hydrolysis and condensation steps. A box has been drawn around the acarviosine grouping present in each case, and the three features that distinguish this group from an equivalent maltose group have been denoted with asterisks. These include a distorted unsaturated ring species, a methyl group in place of an exocyclic hydroxymethyl group, and an N-linked glycosidic bond. The binding subsites in the active site cleft of HPA have been identified according to the convention indicated in the bottom portion of this diagram. Also shown is the expected binding mode for a normal starch substrate, where hydrolysis would occur between subsites −1 and +1.

by HPA. A potential factor in the strong inhibition exhibited by acarbose is the partial planarity of valienamine, whose half-chair conformation mimics the flattened ring of glucose occurring at the transition states (Figure 1).

Although acarbose is an effective inhibitor, its mode of action remains a matter of some controversy. It has been shown by X-ray crystallography that the observed structure of acarbose bound in the active sites of different α-amylases is that of a substantially rearranged product, presumably resulting from a series of enzymatic hydrolysis, condensation, and transglycosylation events (*23*−*30*). These modifications differ but invariably lead to larger and presumably tighter binding inhibitor derivatives, adapted to the particular kinetic and energetic features of the α-amylase involved. For HPA, this inhibitor product is a pseudo-pentasaccharide found in high-affinity binding sites −3 through +2, with the unhydrolyzable acarviosine group spanning the normal site of substrate cleavage between subsites −1 and +1 (Figure 2 and ref *24*). However, to our knowledge, such modified acarbose species have only been seen in the context of crystal soaking experiments, and there has been no direct evidence for such modifications occurring in solution with mammalian α-amylases.

Two acarbose analogues, acarviosine-glucose and isoacarbose, have also been found to bind tightly to mammalian α-amylases (*31*) and can be enzymatically synthesized from acarbose through the action of *Bacillus stearothermophilus* maltogenic amylase (*32*, *33*). Acarviosine-glucose differs from acarbose in having one fewer glucose unit at the reducing end, whereas in isoacarbose, this glucose is attached via an α-(1−6) linkage (Figure 3). Although some limited studies of acarviosine-glucose have been reported (*29*, *31*), the binding mode of isoacarbose is unknown, and therefore, it is not known whether this inhibitor is enzymatically rearranged upon binding in the active sites of mammalian α-amylases.

In this work, we describe kinetic and structural studies of the complexes formed by acarviosine-glucose and isoacar-

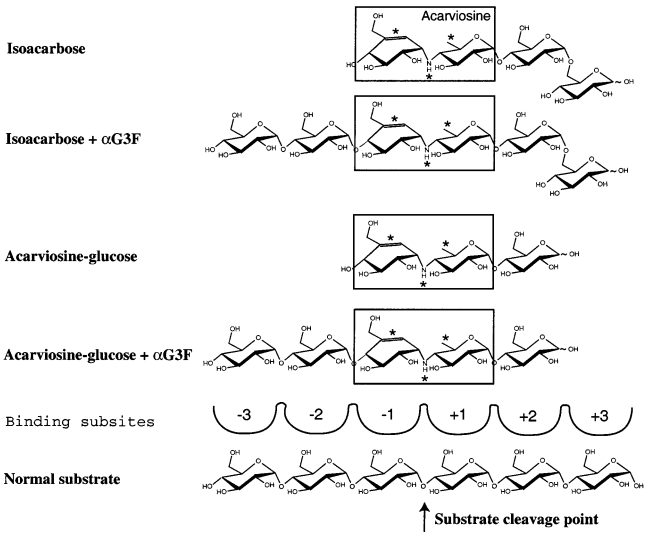

FIGURE 3: Schematic representations of the structures of isoacarbose and acarviosine-glucose as bound to HPA, as well as the conformations of elongated forms produced when these inhibitors are bound in the presence of αG3F. Other conventions used in this drawing are discussed in Figure 2.

bose with HPA, as well as further analyses of elongated forms of these inhibitors. These studies serve to define the binding modes of these inhibitors, the extent of the modifications that are introduced, and those factors involved in the strong observed inhibitory activity. Collectively, the results, along with additional kinetic studies of acarbose action, have led to a proposal defining the pathway by which acarbose is enzymatically optimized upon binding to HPA and a much clearer understanding of the kinetic consequences of this process.

MATERIALS AND METHODS

α-Maltotriosyl fluoride (αG3F) was synthesized according to literature procedures (*34*). 2-Chloro-4-nitrophenyl α-maltotrioside (αCNP-G3) was a kind gift from GelTex Pharmaceuticals. All other buffer chemicals and reagents were obtained from Sigma/Aldrich Canada unless otherwise noted. Recombinant HPA was purified according to literature procedures (*12*).

Kinetic Studies. Human pancreatic α-amylase (HPA) activities were determined in 50 mM sodium phosphate buffer (pH 7.0) containing 100 mM NaCl at 30 °C. Determination of the rate of hydrolysis of αCNP-G3 by HPA was performed by following the increase in the absorbance at 400 nm upon addition of the enzyme (0.0006 mg/mL) in the appropriate buffer over a range of αCNP-G3 concentrations, at each of a series of inhibitor concentrations. These measurements were taken in 1 cm path length cuvettes with a Varian CARY 4000 spectrophotometer attached to a temperature control unit.

The rate of hydrolysis of αG3F was determined by following the increase in the fluoride ion concentration upon addition of the enzyme (0.0002 mg/mL) in the appropriate buffer, over a range of αG3F concentrations, at each of a series of inhibitor concentrations. These measurements were taken using an ORION 96-04 combination fluoride electrode interfaced with a personal computer running LoggerPro.

The data were plotted in the form of a Dixon plot (1/rate vs [inhibitor]). A linear regression fit of each line was performed using GraFit 4.0.21. The K_i value was determined from the intersection of these lines.

Preincubation studies were carried out by incubating the enzyme (final concentration of 0.12 mg/mL) with αG3F (0.2 mM) and/or 20 μM inhibitor for 1 h at 30 °C. Reactions were started with the addition of 10 μL of αCNP-G3 (final concentration of 2.0 mM) and monitored by following the increase in the absorbance at 400 nm.

Structural Studies of Inhibitor Complexes. Acarviosine-glucose and isoacarbose were synthesized following previously reported procedures (*31*). Recombinant wild-type HPA was prepared and crystallized using the hanging drop vapor diffusion method (*24*, *35*). The reservoir solution contained 60% 2-methylpentane-2,4-diol and 100 mM cacodylate at pH 7.5, and the hanging drops consisted of 5 μL of protein solution (16.3 mg/mL) mixed with 5 μL of reservoir solution. Diffraction quality crystals appeared over the period of 1 month. Crystals of complexes of HPA with either acarviosine-glucose or isoacarbose were prepared by soaking HPA crystals in the same crystallization reservoir solution described above, with the addition of 50 mM inhibitor, for 2 h. HPA ternary complexes with these inhibitors and αG3F were prepared by first individually soaking HPA crystals in inhibitor solutions as described, but altered to contain an elevated buffer concentration (160 mM), for 90 min. Following this, a second soak was carried out in the related solution containing 50 mM αG3F instead of the inhibitor, for 15 min.

Diffraction data for all HPA complex crystals were collected on a Mar 345 imaging plate area detector system using Cu Kα radiation supplied by a Rigaku RU300 rotating anode generator operating at 50 kV and 100 mA. The diffraction data that were obtained were processed and reduced with the HKL software package (*36*). The resultant data collection statistics are given in Table 1.

Since crystals of all the HPA complexes were isomorphous with that of the HPA−acarbose complex (*24*), the structure of this latter complex was used as the starting refinement model (with acarbose and water molecules deleted). Refinements were carried out with CNS (*37*). Simulated annealing, and positional and temperature factor refinement, were alternated, and where necessary, the refinement model was manually rebuilt with O (*38*). In the initial stages of structural refinements, the complete polypeptide chain of the refinement model was examined and adjusted on the basis of a composite annealed omit map (with 3% of the residues omitted per segment). Subsequently, the complete polypeptide chain was examined periodically with $F_o - F_c$ and $2F_o - F_c$ difference electron density maps. Following refinement of the polypeptide chain of HPA, bound inhibitors or inhibitor products were positioned on the basis of $F_o - F_c$ difference electron density maps. For all complexes, protein and inhibitor atoms were then jointly refined to obtain the best overall fit. In addition, an *N*-acetylglucosamine moiety was built into observed electron density and refined, to reflect glycosylation of N461 in all complexes. At this point, water molecules were identified from a further $F_o - F_c$ difference electron density map and included in the refinement model if these were able to hydrogen bond to protein atoms, and refined with a thermal factor of <75 Å^2. In a final phase, all protein, inhibitor, and water molecules were jointly refined

Table 1: Structure Determination Statistics

	HPA−Acg	HPA−Acg−αG3F	HPA−Iacb	HPA−Iacb−αG3F
Data Collection Parameters				
space group	$P2_12_12_1$	$P2_12_12_1$	$P2_12_12_1$	$P2_12_12_1$
unit cell dimensions (Å)				
a	52.94	52.85	53.15	52.70
b	68.97	68.92	69.17	69.03
c	131.92	131.99	131.87	132.29
no. of unique reflections	25045	30887	36063	24625
mean $I/\sigma I$[a]	15.9 (4.0)	25.3 (6.3)	21.6 (6.8)	25.2 (9.0)
multiplicity[a]	2.8 (1.9)	8.1 (6.3)	7.5 (3.2)	7.1 (3.0)
R_{merge} (%)[a]	4.5 (15.9)	6.0 (16.0)	6.0 (12.0)	5.3 (13.2)
maximum resolution (Å)	2.0	2.0	1.9	2.2
Structure Refinement Values				
resolution range (Å)	10−2.0	10−2.0	10−1.9	10−2.2
completeness within range (%)[a]	74.9 (49.8)	92.6 (65.4)	93.1 (68.9)	99.0 (98.4)
no. of protein atoms	3946	3946	3946	3946
no. of solvent atoms	164	141	144	133
average *B* factor (Å^2)				
protein atoms	19.4	18.5	21.3	26.1
inhibitor atoms	19.4	18.1	29.3	46.3
solvent atoms	27.1	23.7	26.0	32.6
final *R*-factor/R_{free} (%)[b]	17.4/21.5	17.5/19.9	18.3/19.8	18.6/20.3
Structural Stereochemistry				
rms deviation for bonds (Å)	0.006	0.007	0.006	0.007
rms deviation for angles (deg)	1.2	1.3	1.3	1.4

[a] Values in parentheses refer to the highest-resolution shell (2.07−2.0 Å for HPA−Acg and HPA−Acg−αG3F, 1.97−1.90 Å for HPA−Iacb, and 2.28−2.20 Å for HPA−Iacb−αG3F). [b] Five percent of the diffraction data were kept aside for R_{free}.

to convergence. The final refinement statistics are detailed in Table 1.

RESULTS AND DISCUSSION

Structure of the Isoacarbose−HPA Complex

The structural results clearly indicate that isoacarbose binds tightly in the active site cleft of HPA, with initial difference electron density maps, calculated before the placement of isoacarbose atoms, showing strong continuous density for all four rings of this inhibitor. This is consistent with the strong binding observed for this inhibitor in kinetic studies (Figure 4 and Table 2). Subsequent refinement also shows that, in contrast to what is seen with acarbose, the original tetrasaccharide structure of isoacarbose is preserved in this complex and remains unmodified by the enzyme. As schematically illustrated in Figure 3, the four sugar rings of isoacarbose are bound in subsites −1 through +3 in the active site cleft of HPA.

The overall positioning of bound isoacarbose places this inhibitor immediately adjacent to active site residues D197, E233, and D300 (Figure 5A). The acarviosine moiety of isoacarbose, with its N-linked "glycosidic" bond, binds in subsites −1 and +1, between which cleavage of substrates would normally occur (Figure 3). It is within these two subsites that the majority of hydrogen bond interactions with the inhibitor occur. Strong inhibitor interactions are also found in the +2 binding subsite, but not in the neighboring +3 site in which the terminal α-(1−6)-linked sugar of isoacarbose is bound (Figure 6). These results are consistent with preferred binding/cleavage mode studies which show that there are five primary binding subsites (−3 through +2) that span the active site cleft of HPA (*24*). Kinetic studies further indicate that the more remote −4 and +3 binding subsites have a much lower binding affinity and only become a significant factor in catalysis when longer substrates are bound.

As can be seen in Figure 5A, the +3 binding subsite is indeed at the extremity of one end of the HPA substrate binding cleft. A lower binding affinity at this subsite would serve to explain the higher average thermal factor observed for the terminal α-(1−6)-linked sugar ring bound at this position and the resultant weaker electron density observed for this group. This is the first time that a HPA−inhibitor complex structure has been studied in which this remote binding subsite has been occupied and could therefore be located with some certainty. Nonetheless, it must be remembered that the inhibitor sugar linkage here is α-(1−6), as opposed to the α-(1−4) linkage of a substrate, and therefore, the current inhibitor placement in the +3 binding subsite may only represent in a general fashion the positioning of a normally bound sugar. Alternatively, given that starch does have regular α-(1−6)-linked branches, one role of the HPA +3 binding subsite may be to bind such junctions to facilitate cleavage of the nearby α-(1−4) links. With such a binding capability, one would expect the efficiency of starch degradation to be markedly increased via a reduction in the resultant size of uncleaved products containing α-(1−6) junction points. Follow-up modeling studies to test this idea do indicate that the +3 subsite is sufficiently open to allow a junction point of this type to bind.

As illustrated in Figure 5A, three segments of the polypeptide chain shift in the vicinity of the active site of HPA upon isoacarbose binding. Collectively, two of these segments (residues 148−152 and 237−241) form one side of the +3 and +2 binding subsites and are therefore toward one end of the overall substrate binding cleft. Prominent residues in these segments that make interactions with bound isoacarbose are E240 in subsite +2 and G238 in subsite +3 (see Figure 6). Notably, when isoacarbose binds, the average thermal factors for residues 148−152 and 237−241 decrease from 47 and 42 Å^2 to 27 and 26 Å^2, respectively. These results demonstrate the strong influence that inhibitor binding

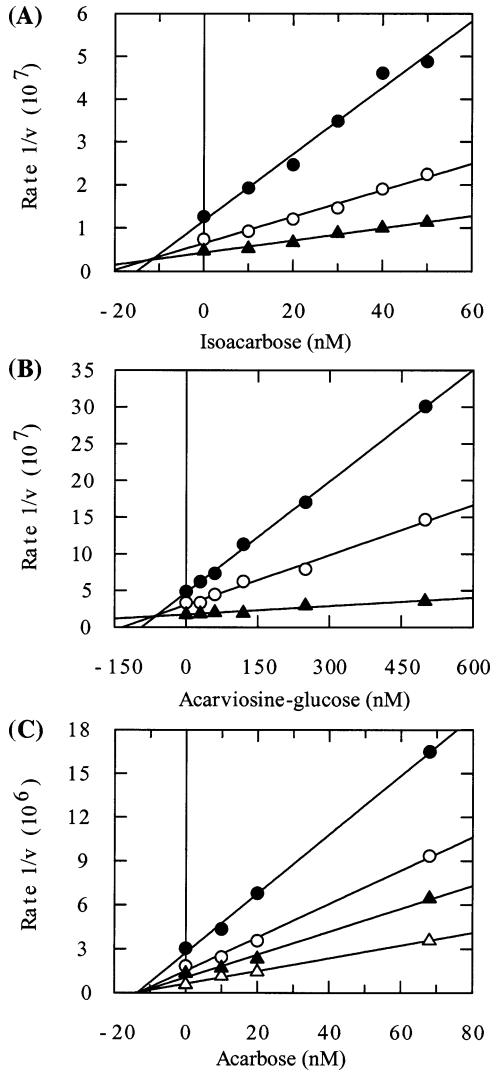

FIGURE 4: Dixon plots showing the rate of hydrolysis of αG3F by HPA in the presence of (A) isoacarbose, (B) acarviosine-glucose, and (C) acarbose. Initial concentrations of αG3F for lines in each plot were as follows: (A) (●) 0.245, (○) 0.625, and (▲) 1.225 mM, (B) (●) 0.1225, (○) 0.245, and (▲) 0.625 mM, and (C) (●) 0.245, (○) 0.625, (▲) 1.225, and (△) 2.45 mM. Samples were not preincubated prior to analysis.

Table 2: K_i Values (μM) for the Inhibition of HPA[a]

inhibitor	αG3F	αCNP-G3	mode of inhibition
isoacarbose	0.012	30	competitive
acarviosine-glucose	0.075	28	competitive
acarbose	0.015	22	noncompetitive

[a] No preincubation of enzyme with inhibitors.

has on the mobility of these two segments of the polypeptide chain.

On the opposite side of the binding cleft, residues 304−309 are found to undergo particularly pronounced shifts to accommodate bound isoacarbose (Figure 5A). These shifts lead to much closer protein−inhibitor contacts over nearly the entire length of the bound inhibitor, including subsites −1 through +3. In wild-type HPA, residues 303−311 are found to form a highly mobile surface loop that is for the most part disordered in electron density maps (*2*). A primary anchor holding this portion of the polypeptide chain to the enzyme surface appears to be catalytic residue D300. Reorientation of this segment of the polypeptide chain in response to isoacarbose binding substantially restricts access to the active site (Figure 5A) and may be a necessary feature in providing the appropriate environment for efficient catalysis when substrates are bound (*24*). It is evident that inhibitor contacts also have a substantial impact on the mobility of this segment of the polypeptide chain from the large drop in the average thermal parameter for these residues, which goes from 55 Å^2 in wild-type HPA to 36 Å^2 in the inhibited enzyme.

Of the three catalytic residues, D197, E233, and D300, it is D300 that is most perturbed by isoacarbose binding. Our results suggest this feature may arise for two reasons. First, D300, along with the neighboring H299, forms very tight interactions with bound isoacarbose in the −1 subsite (Figure 6). It is the sugar ring bound at this subsite that would normally undergo nucleophilic attack by D197 (Figure 1). Particularly notable here is the strong hydrogen bond formed between the side chain of D300 and the NH group of the N-linked glycosidic bond of isoacarbose. Second, the large inhibitor-induced conformational shift of the nearby loop composed of residues 304−309 may be associated with the conformational shift of D300.

Structure of the Acarviosine-Glucose−HPA Complex

Also successful were structural studies designed to determine the bound conformation of acarviosine-glucose in the active site of HPA. As schematically illustrated in Figure 3, the three rings of this inhibitor are bound in subsites −1 through +2. Again this inhibitor is bound in an unmodified form. The overall positioning of acarviosine-glucose parallels that of isoacarbose, with the N-linked glycosidic bond of acarviosine lying between subsites −1 and +1, and in the direct vicinity of active site residues D197, E233, and D300 (Figure 5B). As with the bound conformation of isoacarbose, it appears that the N-linked portion of this inhibitor is acting as a transition state analogue (Figure 1). A comparison of the interactions formed in each binding subsite occupied in common between acarviosine-glucose and isoacarbose indicates that these are comparable (Figure 6). However, the shorter length of acarviosine-glucose (three sugar rings vs the four rings of isoacarbose) does mean that the terminal glucose bound in subsite +2 is much less tightly constrained. This would explain the novel hydrogen bond formed from the O6 hydroxyl of this ring to the O of G306, which is not seen in the isoacarbose complex.

Interestingly, conformational reorientation of the polypeptide chain of HPA in the region of the substrate binding loop (residues 304−309) occurs when acarviosine-glucose binds in the active site cleft. Here again, H305 is brought into binding position even though subsite −2, where it would normally form substrate interactions, is unoccupied. This observation supports our earlier proposal, based on the isoacarbose complex, that the trigger for this movement is the nearby D300, and therefore, reorientation of the substrate binding loop occurs whenever subsites +1 and −1 are occupied.

Comparative Analyses of the Binding Modes of Isoacarbose, Acarviosine-Glucose, and Acarbose

Although acarbose has been the most intensively studied inhibitor of α-amylases, its mode of action remains contro-

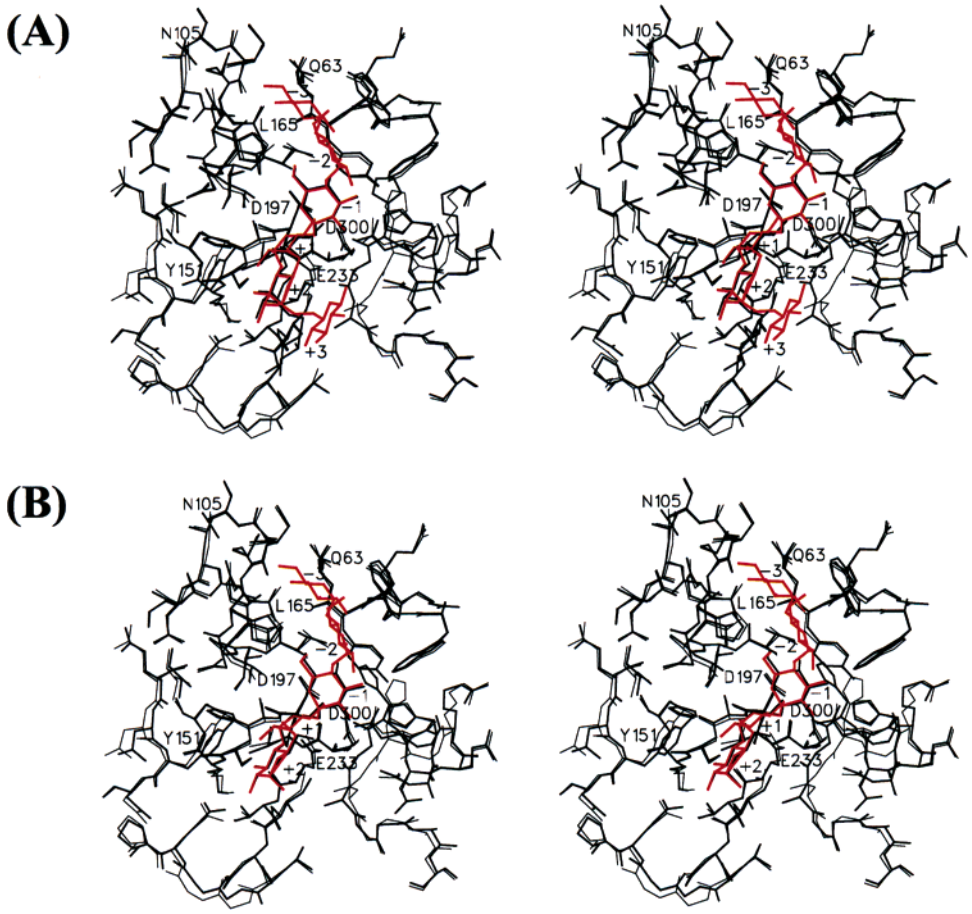

FIGURE 5: Stereo plots of the active site region of HPA in the (A) isoacarbose and (B) acarviosine-glucose complexes (thick black lines). Overlaid in each diagram is the conformation of the polypeptide chain of this region in the free enzyme (thin black lines). Thick red lines show the bound conformation of elongated inhibitors formed in the presence of αG3F. The three active site residues believed to be directly involved in catalytic activity (D197, E233, and D300), along with other residues in the vicinity of the binding cleft, have been labeled. The subsite binding position of each bound inhibitor ring is also indicated according to the scheme presented in Figure 3.

versial largely because, unlike isoacarbose and acarviosine-glucose, it undergoes enzymatic rearrangement upon binding (Figure 2). Comparison of the bound conformation of this observed acarbose product with HPA with that of isoacarbose shows that the interactions are similar in those subsites occupied in common (Figures 5 and 7). The largest observed differences occur at the terminal sugars of each inhibitor and likely relate to their unique occupancy of subsites −3 and −2 in the case of acarbose, and subsite +3 for isoacarbose. Notably, the primary interaction of isoacarbose in subsite +3 is to the carbonyl of G238, which is in fact alternatively positioned away from the active site cleft in the HPA−acarbose complex (Figures 5A and 6).

Acarviosine-glucose and the starting structure of acarbose differ only in acarviosine-glucose being shortened by one glucose unit at the reducing end (Figures 2 and 3). Interestingly, the HPA-rearranged acarbose product that is obtained has had this same glucose removed, in addition to the attachment of a maltose unit to the nonreducing end. Despite their differing sizes, a comparison of rings bound in common (subsites −1 to +2) shows comparable orientations and hydrogen bond interactions. The shorter length of acarviosine-glucose does appear to lead to greater flexibility in binding the terminal +2 glucose unit, which forms a unique interaction with G306 (Figure 5B).

Interestingly, the different subsite binding modes of isoacarbose, acarviosine-glucose, and acarbose induce comparable polypeptide chain shifts. Perhaps most striking is the similar shift in residues 304−309, at the center of which H305 is brought into position to hydrogen bond in the −2 binding subsite. This occurs even though subsite −2 is unoccupied in the isoacarbose and acarviosine-glucose complexes. This provides further evidence that D300, with which all three inhibitors form hydrogen bonds and which forms a part of the structural base from which the substrate binding loop is projected, is the trigger for the movement of this loop, rather than direct loop−inhibitor interactions. Also notably similar in all three inhibitor complex structures are the placements of catalytic residues D197, E233, and D300, indicating that similar conformational responses are elicited directly at the site of catalysis even though different binding subsites are occupied. This would imply that the overall polypeptide chain shifts observed in these complexes are primarily dependent on filling subsites −1 through +2, and that subsites −3, −2, and +3 are less important in this regard.

Resistance of Isoacarbose and Acarviosine-Glucose to Enzymatic Rearrangement

A key difference distinguishing acarbose from acarviosine-glucose and isoacarbose is the complete lack of enzymatic rearrangement of the latter inhibitors. This phenomenon would appear to be in large part due to the substrate cleavage pattern of HPA. Product analyses of G3−G7 demonstrate that the final hydrolysis products that are obtained are

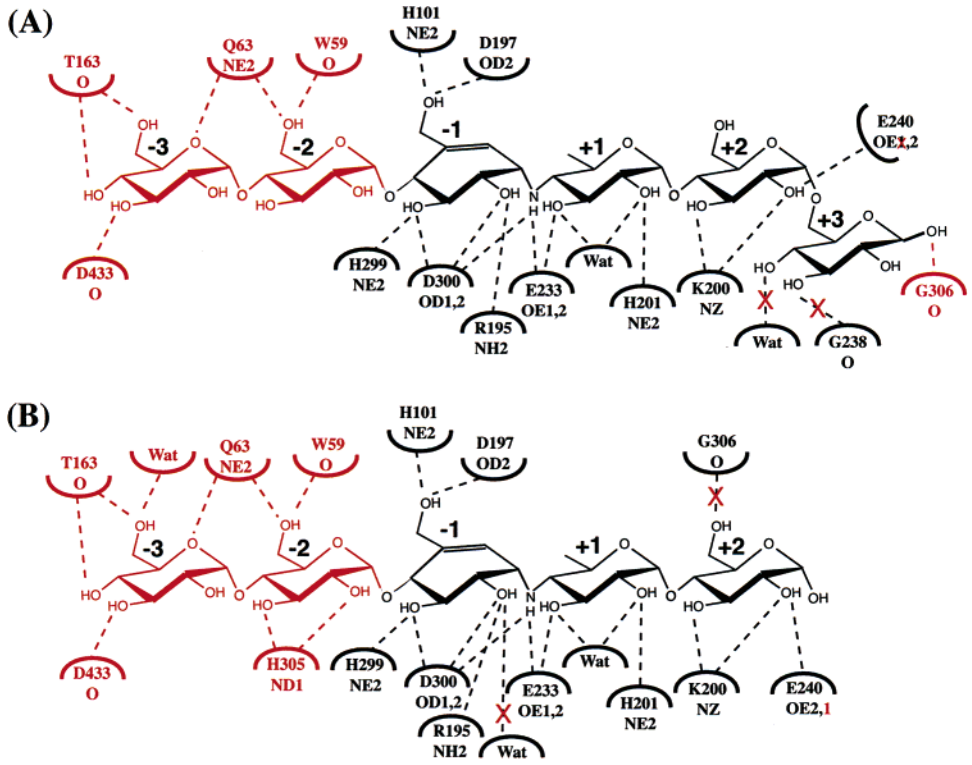

FIGURE 6: Diagrammatic representation of the hydrogen bond interactions formed with (A) isoacarbose and (B) acarviosine-glucose when bound in the active site of HPA. Shown in red are the additional glucose units added to these inhibitors when bound in the presence of αG3F. Additional or altered interactions found for elongated forms are also shown in red. Red times signs (×) indicate specific interactions that are not present in the elongated form. The subsites in which individual rings are bound are labeled (also see Figure 3).

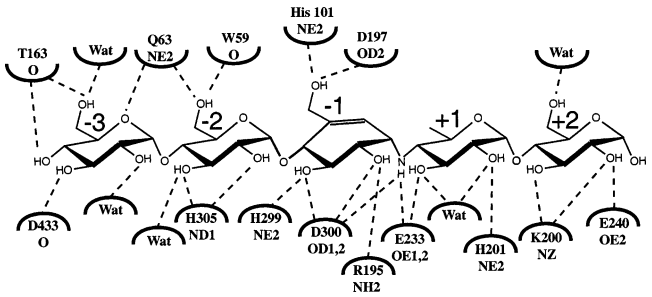

FIGURE 7: Hydrogen bond interactions formed by the enzymatically rearranged product of acarbose when bound in the active site of HPA. Those binding subsites filled by the modified inhibitor are labeled.

predominantly G2 and G3 (*24*). In addition, G3 is found to be a very poor substrate for HPA (*13*). Therefore, the resistance of acarviosine-glucose to hydrolysis appears to be related to both the limited activity of HPA toward cleavage of maltotriose, as well as the fact that two of the sugar rings of this inhibitor are joined by an uncleavable N-linked glycosidic bond (Figure 3). It is also likely that the tighter binding of the transition state-like acarviosine group in subsites −1 and +1 substantially reduces the probability that the normal α-(1−4) linkage to the alternative glucose unit would be positioned next to catalytic residues.

The complete absence of isoacarbose hydrolysis is surprising given how HPA readily cleaves maltotetraose to give mainly maltose and a smaller amount of glucose. The hydrolytic resistance of the α-(1−4) link between acarviosine and the neighboring glucose could arise for several reasons. It is possible that the nearby proximity of the acarviosine group is a factor. This is supported by the observation that the equivalent bond in acarviosine-glucose also cannot be cleaved. It is also likely that the α-(1−6) linkage to the terminal glucose in isoacarbose precludes the positioning of this group in the +2 binding subsite where it must be bound for cleavage to occur at the α-(1−4) linkage between acarviosine and the adjacent glucose. Indeed, modeling studies show unfavorable structural conflicts develop if an α-(1−6)-linked glucose is placed in the +2 binding subsite.

Potential Pathways of Acarbose Rearrangement by HPA

A long-standing puzzle in the study of acarbose action is how this inhibitor is specifically rearranged by HPA in the absence of other reactants (Figure 2). Our current results with the unmodified acarviosine-glucose and isoacarbose inhibitors provide clear boundaries with respect to the probable sequence of enzymatic reactions involved. For acarviosine-glucose, it is apparent that the α-(1−4) link between acarviosine and glucose cannot be cleaved by HPA. This suggests that bond cleavage between acarviosine and the neighboring glucose in acarbose is unlikely to occur as well.

Notably, the longer isoacarbose inhibitor is also resistant to modification due to the presence of an α-(1−6) link to its terminal glucose (Figure 3). As the only difference between the inhibitors is in this terminal linkage to glucose, the implication is that the comparable α-(1−4) link between terminal glucoses in acarbose can and must be cleaved, as the first step in enzymatic rearrangement of acarbose. It is also evident, on the basis of the final observed acarbose product, that there must be additional enzymatic steps carried out by HPA when acarbose is bound.

The subsequent steps in any potential pathways by which the overall enzymatic rearrangement of acarbose might occur by HPA are severely limited by three factors. The first is

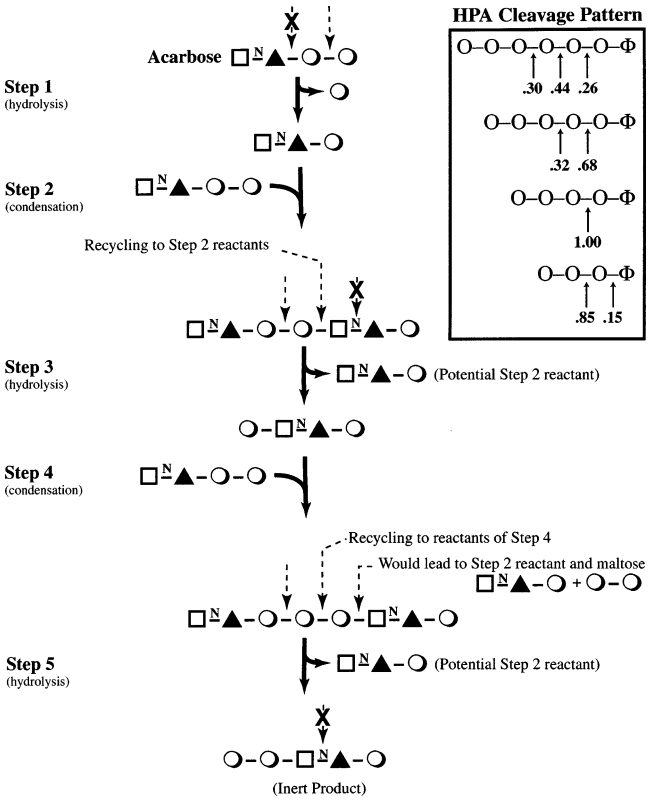

FIGURE 8: Proposed five-step pathway by which acarbose is enzymatically rearranged by HPA through a series of hydrolysis and condensation steps. Dashed arrows indicate expected cleavage points in pathway intermediates. The final pseudo-pentasaccharide product is inert to further alterations, since the unhydrolyzable N-linked glycosidic bond of the acarviosine group present spans the only available cleavage point. All five high-affinity binding subsites (−3 to +2) are occupied when the final product is bound. The inset at the top right is the observed cleavage pattern of HPA for substrates of varying sizes, along with the frequency with which such cleavages occur (see ref *24* for further details).

that the only "substrates" available for transglycosylations and condensations in this process are the initial acarviosine-glucose product discussed above and acarbose itself. The glucose produced along with acarviosine-glucose is too poor as a substrate to be a factor. Second, HPA exhibits a very specific pattern of cleavages on substrates of differing lengths, which considerably delimits the range of products obtained (Figure 8). Finally, it seems that at least two of the linkages in acarbose cannot be hydrolyzed by HPA, and this therefore further limits the range of available products. Within these three restrictions, it is possible to outline the simplest sequence of enzymatic reactions likely involved when acarbose binds to HPA. This is summarized in Figure 8, and supporting explanations for each of the five steps involved are provided below.

Step 1 is the initial hydrolysis of acarbose to acarviosine-glucose and glucose, occurring at the only bond upon which HPA can act.

Step 2 is elongation of the acarviosine-glucose product of step 1. This can only occur by condensation with acarbose. Our current studies show that condensation of two acarviosine-glucoses either does not occur or is alternatively hydrolyzed back to acarviosine-glucose as prescribed by the cleavage specificity of HPA.

Step 3 is the result of HPA cleavage preferences for maltoheptaose at three bonds. For the product of step 2, cleavage between the two rings of the acarviosine unit is not possible, while the second preferred mode of cleavage would simply produce the original reactants of step 2. The third and productive cleavage would result in an intermediate elongated by one glucose unit on the nonreducing end.

Step 4 is a second acarbose condensation to the intermediate produced in step 3 to give a pseudo-octasaccharide.

Step 5 is like step 3, in which HPA could potentially cleave the product of step 4 at three locations. One of these would simply produce the initial reactants of step 4, while the cleavage point closest to the reducing end would result in acarviosine-glucose and maltose, after subsequent cleavages. Significantly, the third cleavage point would produce the mature rearranged acarbose product and acarviosine-glucose. No further processing of the mature pseudo-pentasaccharide acarbose product is expected since HPA exclusively cleaves maltopentaose into maltotriose and maltose. This particular bond is an uncleavable N-linked glycosidic bond in the product that is obtained.

Notably, it seems that a minimum of five enzymatic steps are required to arrive at the final inert acarbose product. This includes two condensation reactions involving the starting form of acarbose, and it is only this form that is usable as an elongation agent because of the specific cleavage pattern of HPA. Condensation reactions in water are, in general, highly unfavorable thermodynamically. In this case, however, the high binding affinity of the end product is sufficient to outweigh the thermodynamic costs. Interestingly, all the cleavage byproducts that are produced are either the reactants of the previous condensation step and can therefore be recycled into the elongation process or acarviosine-glucose, the original precursor of the overall reaction scheme, which can be used to initiate further elongation sequences. The minor glucose and maltose products are poor substrates for HPA and thus unlikely to play any further role. Importantly, the overall elongation process does not produce unusable high-affinity byproducts that could potentially accumulate and compete for the active site of HPA. This conclusion agrees with structural studies, where only the pseudo-pentasaccharide acarbose product is found bound in the active site of HPA.

Thus, according to the proposed sequence of events, the structure of the final bound product that is obtained results from a combination of factors. These include the unhydrolyzable nature of the two glycosidic linkages found in acarbose, the mimicry of the acarviosine group of the transition state, the occupancy of all five high-affinity binding sites, and the cleavage pattern of HPA.

Elongation of Isoacarbose and Acarviosine-Glucose

A key finding of our work is that, unlike acarbose, neither isoacarbose nor acarviosine-glucose is elongated or rearranged upon binding to HPA. This appears to result from the inability of HPA to cleave glucose residues from the reducing terminus of these inhibitors. Nonetheless, it seemed to be probable to us that the equivalent elongation could be achieved by coaddition of an activated glycosyl fluoride donor. Therefore, as part of an overall strategy to explore optimization of inhibitor length and binding affinity, we have tested the possibility of elongating both isoacarbose and acarviosine-glucose by "*in situ*" transglycosylation. These experiments were conducted by mixing the substrate αG3F

with each inhibitor in the presence of HPA in the crystalline state. αG3F is an activated maltotriosyl derivative wherein the anomeric hydroxyl group has been replaced with fluorine, a much better leaving group (*13*). The structures of the resultant inhibitor products were then resolved using X-ray diffraction techniques.

As the structural results summarized in Figures 3, 5, and 6 indicate, these elongation experiments were successful. For isoacarbose, reaction with αG3F leads to the addition of a maltose unit onto the nonreducing end of this inhibitor, with the extra glucose rings bound in subsites −2 and −3 (Figure 5A). Notably, that portion of this inhibitor product representing the original structure of isoacarbose is bound as before, in subsites −1 to +3 (Figure 3). As observed for isoacarbose by itself, the overall final subsite positioning scheme of the elongated inhibitor product in the active site cleft of HPA appears to be mandated by two factors. The first involves the restriction of only being able to accommodate an α-(1−6)-linked glucose in subsite +3. The second is the placement of the transition state analogue acarviosine grouping with its N-linked glycosidic bond between subsites −1 and +1. This latter feature would also serve to terminate any further enzymatic cleavage or elongation reactions with the bound inhibitor product.

As illustrated in Figure 6, a comparable set of hydrogen bond interactions with the original isoacarbose group of the elongated version of this inhibitor in subsites −1 through +2 are found. However, the α-(1−6)-linked glucose unit bound in subsite +3 is shifted in the elongated inhibitor in comparison to its position when isoacarbose is bound alone (Figure 5A). This leads to the formation of alternative hydrogen bond interactions with G306, and the loss of interactions with G238 and a water molecule. Also affected is the interaction of the side chain of E240 in the +2 subsite. It would seem that the multiple, well-defined hydrogen bonds formed by the additional maltosyl moiety of the elongated inhibitor in the −2 and −3 subsites (although not H305 in this case) mediate the positional shifts observed in the +3 subsite. This likely occurs through interactions with the substrate binding loop composed of residues 303−311, which undergoes a substantial reorientation upon binding the elongated inhibitor (Figure 5A).

It is possible that the elongation pathway that is involved is similar to that outlined for acarbose in Figure 8, such that a maltotetraose (G4) substrate would be added to the nonreducing end of isoacarbose in an initial step. The source of this G4 is likely to be the original reactant αG3F, which has been shown to react with itself in the presence of HPA to produce αG6F, which is subsequently cleaved by the enzyme to yield G4 and G2F (Figure 8 and ref *13*). However, an alternative elongation pathway would also seem possible in this case since both G4 and αG2F can serve as activated maltosyl donors to directly append the maltosyl group to isoacarbose as they have almost identical k_{cat}/K_m values (*24*). Supportive evidence for this mode of isoacarbose elongation arises from additional experiments that demonstrate that equivalent elongation does not occur in the presence of maltotriose. This substrate has a normal anomeric hydroxyl group but exhibits little activity with HPA, and unlike αG3F, it has no activated leaving group. A similar lack of isoacarbose elongation is observed with the less reactive substrates maltose and glucose. On the other hand, maltotetraose is readily utilized by HPA to elongate isoacarbose to the same product as observed with αG3F (Figure 3).

Analysis of the elongation reaction product obtained for acarviosine-glucose shows a similar pattern of results. Here, reaction with αG3F also leads to the addition of a maltosyl unit to the nonreducing end of acarviosine-glucose, to give an extended inhibitor that binds in subsites −3 to +2 (Figure 3). Retaining its position in subsites −1 to +2 is that portion representing the original acarviosine-glucose. Reflecting the additional conformational restraints of binding a longer inhibitor, the acarviosine ring in subsite −1 is slightly adjusted relative to its position when only acarviosine-glucose is bound, causing the loss of a water molecule interaction (Figures 5B and 6). This also leads to small differences in the nature of the shift of the substrate binding loop and its interactions in subsite +2.

As with isoacarbose, the elongation product obtained for acarviosine-glucose must be the result of a number of catalytic events. Also similar is the fact that maltotriose, maltose, and glucose are ineffective reactants, whereas αG3F and maltotetraose give the same elongation product. These data strongly support the conclusion that the pathway for acarviosine-glucose elongation is the same as that of isoacarbose.

What Is the Real Meaning of Observed Inhibition Kinetics for Acarbose and Related Analogues?

In light of the structural results obtained for all three inhibitors, it should be possible to detect their elongation and/or rearrangement kinetically if indeed the product molecules are tighter binding species. This would necessitate the choice of a substrate that is monitored with high sensitivity, but which only slowly (on the time scale of the experiment) transglycosylates onto the added inhibitor. An excellent candidate for this role is αCNP-G3, whose hydrolysis can be detected by UV−vis spectrophotometry, but whose k_{cat} value ($k_{cat} = 2.98\ s^{-1}$) is considerably lower than that for maltosyl fluoride ($k_{cat} = 150\ s^{-1}$) or maltotriosyl fluoride ($k_{cat} = 285\ s^{-1}$).

Accordingly, the set of experiments shown in Figure 9 was first performed with acarbose, which is known to undergo an elongation and rearrangement process. As can be seen from the progress curves, coaddition of or preincubation with αG3F (0.2 mM) results in identical, lower, rates, presumably due to competitive inhibition by the (nonchromogenic) substrate and/or its transglycosylation/hydrolysis products. The fact that identical rates were seen with and without preincubation suggests that, under these conditions, the αG3F reaction has reached its steady state very quickly.

As might be expected, a greater level of inhibition was seen when acarbose (0.020 mM) was added, and indeed, a K_i value of 22 μM was measured for acarbose using αCNP-G3 as the substrate (Table 2). This is a considerably higher value than that reported for acarbose previously when measured against other substrates (*13*, *25*−*28*, *33*). Preincubation, however, yielded a somewhat greater level of inhibition, presumably due to elongation of the inhibitor by αCNP-G3. Indeed, closer inspection of the plot in the absence of preincubation reveals significant curvature, resulting from this *in situ* formation of a better inhibitor. The strongest inhibition, however, was seen when αG3F was also included in the reaction mixture, with rates being decreased

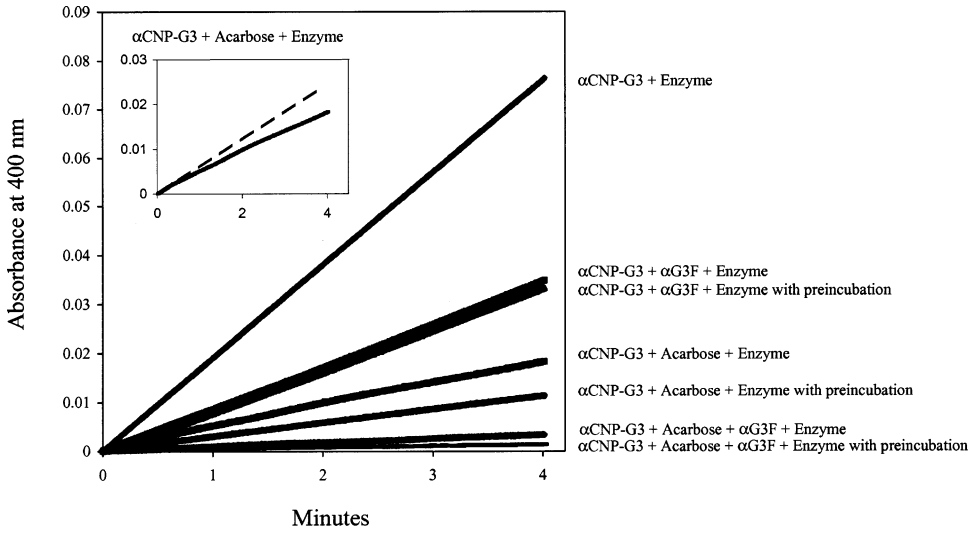

FIGURE 9: Rate of hydrolysis of αCNP-G3 by HPA in the absence and presence of acarbose, without or with various preincubation criteria. Specific reactants used in each experiment are listed to the right of this plot, and all preincubations were carried out for 1 h. The inset demonstrates the significant curvature of the line (—) corresponding to αCNP-G3 hydrolysis by HPA in the presence of acarbose without preincubation. For comparison, the initial trend for αCNP-G3 hydrolysis under these conditions is shown (— — —). The observed line curvature suggests the growing influence of elongated and tighter binding inhibitor forms. See the Supporting Information for related plots involving isoacarbose and acarviosine-glucose. These show results similar to those obtained for acarbose.

a further 4-fold. Preincubation, which presumably leads to even more elongation, results in a yet-lower rate. Similar results were seen with acarviosine-glucose and isoacarbose (results not shown; see the Supporting Information). In each case, a substantially greater level of inhibition was observed and the inhibition was enhanced by preincubation. Table 2 summarizes the kinetic values that were obtained.

It is important to note that this apparent slow binding differs from that commonly seen with other tight-binding inhibitors, where it is believed that a conformational change of the enzyme is required before the final binding mode is achieved. The fact that apparent slow binding is only seen here with "slow" substrates such as αCNP-G3 and not with "fast" substrates such as αG3F distinguishes the two situations. To assess these different inhibitory modes, K_i values were determined for each inhibitor using αCNP-G3 as the substrate, taking initial rates before much transglycosylation could occur, and also using αG3F as the substrate, when inhibition would reflect, to a large extent, the elongated inhibitor (Table 2).

These results conclusively demonstrate that the inhibitor elongation induced in structural studies is also occurring in solution. It is also clear that the K_i value determined using αG3F is an apparent K_i value of a modified inhibitor or a mixture of inhibitors. In contrast, the K_i value determined using αCNP-G3 most likely represents a more accurate assessment of the K_i value of the unmodified inhibitor. Interestingly, the k_{cat} values for hydrolysis of malto-oligosaccharides and starch are similar to that of αG3F (*13*); thus, K_i values measured using starch-based substrates also reflect the elongation species. Acarbose will also be elongated upon co-incubation with such substrates and HPA. Since malto-oligosaccharides are present in the human intestine, this elongation reaction will probably take place when acarbose is ingested with such substrates. Therefore, it is likely that in the human body, the inhibitory form of acarbose is indeed an elongated species with K_i values similar to those seen in the literature and herein when αG3F is used as the substrate (Table 2).

ACKNOWLEDGMENT

We thank Yili Wang for technical assistance.

SUPPORTING INFORMATION AVAILABLE

Additional kinetic data plots showing the rate of hydrolysis of αCNP-G3 by HPA in the absence and presence of isoacarbose and acarviosine-glucose, without or with various preincubation criteria. This material is available free of charge via the Internet at http://pubs.acs.org.

REFERENCES

1. Berman, H. M., Westbrook, J., Feng, Z., Gilliland, G., Bhat, T. N., Weissig, H., Shindyalov, I. N., and Bourne, P. E. (2000) The Protein Data Bank, *Nucleic Acids Res. 28*, 235−242.
2. Brayer, G. D., Luo, Y., and Withers, S. G. (1995) The structure of human pancreatic α-amylase at 1.8 Å resolution and comparisons with related enzymes, *Protein Sci. 4*, 1730−1742.
3. Feller, G., le Bussy, O., Houssier, C., and Gerday, C. (1996) Structural and functional aspects of chloride binding to *Alteromonas haloplanctis* α-amylase, *J. Biol. Chem. 271*, 23836−23841.
4. Levitzki, A., and Steer, M. L. (1974) The allosteric activation of mammalian α-amylase by chloride, *Eur. J. Biochem. 41*, 171−180.
5. Numao, S., Maurus, R., Sidhu, G., Wang, Y., Overall, C. M., Brayer, G. D., and Withers, S. G. (2002) Probing the role of the chloride ion in the mechanism of human pancreatic α-amylase, *Biochemistry 41*, 215−225.
6. Gumucio, D. L., Wiebauer, K., Caldwell, R. M., Samuelson, L. C., and Meisler, M. H. (1988) Concerted evolution of human amylase genes, *Mol. Cell. Biol. 8*, 1197−1205.
7. Nishide, T., Emi, M., Nakamura, Y., and Matsubara, K. (1986) Corrected sequences of cDNAs for human salivary and pancreatic α-amylases, *Gene 50*, 371−372.
8. Ramasubbu, N., Paloth, V., Luo, Y., Brayer, G. D., and Levine, M. J. (1996) Structure of Human Salivary α-Amylase at 1.6 Å Resolution: Implications for its Role in the Oral Cavity, *Acta Crystallogr. D52*, 435−446.
9. Henrissat, B. (1991) A classification of glycosyl hydrolases based on amino acid sequence similarities, *Biochem. J. 280*, 309−316.
10. Henrissat, B., Callebaut, I., Fabrega, S., Lehn, P., Mornon, J. P., and Davies, G. (1995) Conserved catalytic machinery and the prediction of a common fold for several families of glycosyl hydrolases, *Proc. Natl. Acad. Sci. U.S.A. 92*, 7090−7094.
11. Braun, C., Brayer, G. D., and Withers, S. G. (1995) Mechanism-based inhibition of yeast α-glucosidase and human pancreatic

α-amylase by a new class of inhibitors, *J. Biol. Chem. 270*, 26778−26781.
12. Rydberg, E. H., Sidhu, G., Vo, H. C., Hewitt, J., Côté, H. C. F., Wang, Y., Numao, S., MacGillivray, R. T. A., Overall, C. M., Brayer, G. D., and Withers, S. G. (1999) Cloning, mutagenesis, and structural analysis of human pancreatic α-amylase expressed in *Pichia pastoris*, *Protein Sci. 8*, 635−643.
13. Rydberg, E. H., Li, C., Maurus, R., Overall, C. M., Brayer, G. D., and Withers, S. G. (2002) Mechanistic analyses of catalysis in human pancreatic α-amylase: Detailed kinetic and structural studies of mutants of three conserved carboxylic acids, *Biochemistry 41*, 4492−4502.
14. Truscheit, E., Frommer, W., Junge, B., Muller, L., Schmidt, D. D., and Wingender, W. (1981) Chemistry and Biochemistry of Microbial α-Glucosidase Inhibitors, *Angew. Chem., Int. Ed. Engl. 20*, 744−761.
15. Noda, K., Umeda, F., and Nawata, H. (1997) Effect of acarbose on glucose intolerance in patients with non-insulin-dependent diabetes mellitus, *Diabetes Res. Clin. Pract. 37*, 129−136.
16. Clissold, S. P., and Edwards, C. (1988) Acarbose. A preliminary review of its pharmacodynamic and pharmacokinetic properties, and therapeutic potential, *Drugs 35*, 214−243.
17. Brogard, J. M., Willemin, B., Blickle, J. F., Lamalle, A. M., and Stahl, A. (1989) α-Glucosidase inhibitors: A new therapeutic approach in diabetes and functional hypoglycemia, *Rev. Med. Interne. 10*, 365−374.
18. Hiele, M., Ghoos, Y., Rutgeerts, P., and Vantrappen, G. (1992) Effects of acarbose on starch hydrolysis. Study in healthy subjects, ileostomy patients, and in vitro, *Dig. Dis. Sci. 37*, 1057−1064.
19. Thornton, J., Dryden, A., Kelleher, J., and Losowsky, M. (1986) Does super efficient starch absorption promote diverticular disease? *Br. Med. J. 292*, 1708−1710.
20. Thornton, J., Dryden, A., Kelleher, J., and Losowsky, M. (1987) Super-efficient starch absorption. A risk factor for colonic neoplasia? *Dig. Dis. Sci. 32*, 1088−1091.
21. Scannapieco, F. A., Bhandary, K., Ramasubbu, N., and Levine, M. J. (1990) Structural relationship between the enzymatic and streptococcal binding sites of human salivary α-amylase, *Biochem. Biophys. Res. Commun. 173*, 1109−1115.
22. Scannapieco, F. A., Torres, G., and Levine, M. J. (1993) Salivary α-amylase: Role in dental plaque and caries formation, *Crit. Rev. Oral Biol. Med. 4*, 301−307.
23. Qian, M., Haser, R., Buisson, G., Duée, E., and Payan, F. (1994) The active center of a mammalian α-amylase. Structure of the complex of a pancreatic α-amylase with a carbohydrate inhibitor refined to 2.2 Å resolution, *Biochemistry 33*, 6284−6294.
24. Brayer, G. D., Sidhu, G., Maurus, R., Rydberg, E., Braun, C., Wang, Y., Nguyen, N., Overall, C., and Withers, S. G. (2000) Subsite mapping of the human pancreatic α-amylase active site through structural, kinetic, and mutagenesis techniques, *Biochemistry 39*, 4778−4791.
25. Gilles, C., Astier, J. P., Marchis-Mouren, G., Cambillau, C., and Payan, F. (1996) Crystal structure of pig pancreatic α-amylase isoenzyme II, in complex with the carbohydrate inhibitor acarbose, *Eur. J. Biochem. 238*, 561−569.
26. Brzozowski, A. M., and Davies, G. J. (1997) Structure of the *Aspergillus oryzae* α-amylase complexed with the inhibitor acarbose at 2.0 Å resolution, *Biochemistry 36*, 10837−10845.
27. Kadziola, A., Sogaard, M., Svensson, B., and Haser, R. (1998) Molecular structure of a barley α-amylase-inhibitor complex: Implications for starch binding and catalysis, *J. Mol. Biol. 278*, 205−217.
28. Brzozowski, A. M., Lawson, D. M., Turkenburg, J. P., Bisgaard-Frantzen, H., Svendsen, A., Borchert, T. V., Dauter, Z., Wilson, K. S., and Davies, G. J. (2000) Structural analysis of a chimeric bacterial α-amylase. High-resolution analysis of native and ligand complexes, *Biochemistry 39*, 9099−9107.
29. Qian, M., Nahoum, V., Bonicel, J., Bischoff, H., Henrissat, B., and Payan, F. (2001) Enzyme-catalyzed condensation reaction in a mammalian α-amylase. High-resolution structural analysis of an enzyme−inhibitor complex, *Biochemistry 40*, 7700−7709.
30. Aghajari, N., Roth, M., and Haser, R. (2002) Crystallographic evidence of a transglycosylation reaction: ternary complexes of a psychrophilic α-amylase, *Biochemistry 41*, 4273−4280.
31. Kim, M., Lee, S., Lee, H., Lee, S. Y., Baek, J., Kim, D., Moon, T., Robyt, J. F., and Park, K. (1999) Comparative study of the inhibition of α-glucosidase, α-amylase, and cyclomaltodextrin glucanosyltransferase by acarbose, isoacarbose, and acarviosine-glucose, *Arch. Biochem. Biophys. 371*, 277−283.
32. Cha, H. J., Yoon, H. G., Kim, Y. W., Lee, H. S., Kim, J. W., Kweon, K. S., Oh, B. H., and Park, K. H. (1998) Molecular and enzymatic characterization of a maltogenic amylase that hydrolyzes and transglycosylates acarbose, *Eur. J. Biochem. 253*, 251−262.
33. Park, K. H., Kim, M. J., Lee, H. S., Han, N. S., Kim, D., and Robyt, J. F. (1998) Transglycosylation reactions of *Bacillus stearothermophilus* maltogenic amylase with acarbose and various acceptors, *Carbohydr. Res. 313*, 235−246.
34. Junnemann, J., Thiem, J., and Pedersen, C. (1993) Facile synthesis of acetylated glycosyl fluorides derived from di- and tri-saccharides, *Carbohydr. Res. 249*, 91−94.
35. Burk, D., Wang, Y., Dombroski, D., Berghuis, A., Evans, S. V., Luo, Y., Withers, S. G., and Brayer, G. D. (1993) Isolation, crystallization and preliminary diffraction analyses of human pancreatic α-amylase, *J. Mol. Biol. 230*, 1084−1085.
36. Otwinowski, Z., and Minor, W. (1997) Macromolecular crystallography, Part A, *Methods Enzymol. 276*, 307−326.
37. Brünger, A. T., Adams, P. D., Clore, G. M., DeLano, W. L., Gros, P., Grosse-Kunstleve, R. W., Jiang, J.-S., Kuszewski, J., Nilges, M., Pannu, N. S., Read, R. J., Rice, L. M., Simonson, T., and Warren, G. L. (1998) Crystallography & NMR system (CNS): A new software system for macromolecular structure determination, *Acta Crystallogr. D54*, 905−921.
38. Jones, T. A., Zhou, J.-Y., Cowan, S. W., and Kjeldgaard, M. (1991) Improved methods for building protein models in electron density maps and the location of errors in these models, *Acta Crystallogr. A47*, 110−119.

BI048334E